

HANGING NODES IN THE UNIFYING THEORY OF A POSTERIORI FINITE ELEMENT ERROR CONTROL*

C. Carstensen

*Institut für Mathematik, Humboldt Universität zu Berlin,
Rudower Chaussee 25, D-12489 Berlin, Germany
Email: cc@mathematik.hu-berlin.de*

Jun Hu

*LMAM and School of Mathematical Sciences, Peking University, Beijing 100871, China
Email: hujun@math.pku.edu.cn*

Abstract

A unified a posteriori error analysis has been developed in [18, 21–23] to analyze the finite element error a posteriori under a universal roof. This paper contributes to the finite element meshes with hanging nodes which are required for local mesh-refining. The two-dimensional 1-irregular triangulations into triangles and parallelograms and their combinations are considered with conforming and nonconforming finite element methods named after or by Courant, Q_1 , Crouzeix-Raviart, Han, Rannacher-Turek, and others for the Poisson, Stokes and Navier-Lamé equations. The paper provides a unified a priori and a posteriori error analysis for triangulations with hanging nodes of degree ≤ 1 which are fundamental for local mesh refinement in self-adaptive finite element discretisations.

Mathematics subject classification: 65N10, 65N15, 35J25.

Key words: A posteriori, A priori, Finite element, Hanging node, Adaptive algorithm.

1. Introduction

More and more accurate scientific simulations in less and less CPU time on smaller and smaller computational resources are one important new feature in natural sciences, engineering, medicine, and business with huge impact on our modern technological societies. The presently most important area of worldwide scientific activities in the design of more effective and accurate numerical predictions in the computational sciences is the proper mesh-design within the discretisation of partial differential or integral equations.

Nonconforming finite element methods on parallelograms are of particular attraction in computational fluid and solid mechanics because of their conservation properties. Their application in adaptive local mesh-refining algorithms, however, involves a partition with triangles or with hanging nodes of at least first order. This paper is devoted to a universal a priori and a posteriori error analysis for those 1-irregular meshes specified in Section 2 below. Tables 1.1 and 1.2 display practical solutions for the Laplace, Stokes and Navier Lamé equations problem discussed in this paper.

At first glance, the concept of hanging nodes appears straightforward: If a vertex x of a finite element domain (with polygonal boundary) belongs to the interior of an edge E (of another element domain) in the sense that it is a nontrivial convex combination of the end points of E , then z is called a hanging node. However, in case of continuous discrete functions, the

* Received February 23, 2008 / Revised version received May 18, 2008 / Accepted May 20, 2008 /

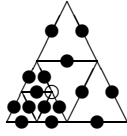
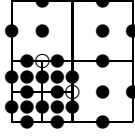
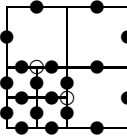
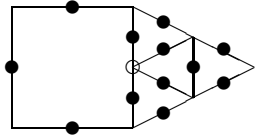
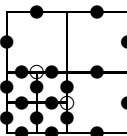
Table 1.1: FEMs with hanging nodes: bullets mark the degrees of freedom and circles mark hanging nodes subject to internal restrictions.

illustration	reference	illustration	reference
	Courant		Q_1
	[27]		[32]
	[37]		Wilson [38]
	[30]		CNR [34]

organization of the degrees of freedom is not too easy. Many authors assume a master-slave concept in the sense that there are free nodes and the hanging nodes follow by interpolation. Fig. 1.1 displays some mesh which, in case of continuous discrete functions and vanishing Dirichlet boundary conditions, has not a single free node. Moreover, the concept of parents and children is not immediate here. Hence, at second glance, the concept of hanging nodes is associated with a hierarchy of discretisations and so a sequence of meshes. This is outlined in Section 2 with definitions of concepts like 1-irregular meshes and associated conforming and nonconforming first-order finite element spaces.

Throughout the paper, we discuss five assumptions (A1)-(A5) which we comment very briefly

Table 1.2: FEMs with hanging nodes: bullets mark the degrees of freedom and circles mark hanging nodes subject to internal restrictions.

illustration	reference	illustration	reference
	[27]		Han [32]
	NR [37]		
	[30]		

on in the sequel:

- (A1) states that the meshes are obtained by red-refinement and thereby hanging nodes are produced in a very structured way.
- (A2) states that the integral means of the jumps along some edges vanish. This is obvious for conforming discrete functions and standard for nonconforming ones.
- (A3) assumes the existence of some Fortin interpolation operator into the discrete space V_h with conservation and stability properties.
- (A4) assumes the existence of a discrete stress field based on the discrete solutions u_h and p_h which serves in the residual error estimators.
- (A5) assumes the existence of a local operator from [22, 23] with elementwise conservation properties for the a posteriori error analysis.

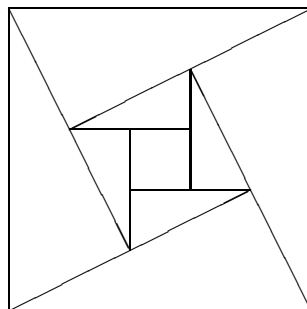


Fig. 1.1. Mesh excluded from this paper as it is not partly red-refined from some regular mesh \mathcal{T}_0 . The degree of hanging nodes in the displayed mesh is hard to specify and patches of free nodes can contain an unbounded number of elements (since the figure can be extended in a self-similar sense).

The assumptions (A1)-(A5) guarantee compactly-supported nodal basis functions and optimal a priori convergence rates for the consistency error. They allow for an application of the unifying theory of a posteriori finite element error control and thereby allow for a unified analysis for a large class of finite element technologies and applications.

The outline of the remaining part of paper is as follows: Section 2 introduces irregular triangulations with (A1) and provides a main approximation result. The a priori error analysis is given in an abstract format in Section 3 under conditions (A2)-(A3) which we regard as fairly weak but to allow for optimal a priori convergence rates for the consistency error, compactly-supported nodal basis functions, and Assumption (A5). Section 4 is devoted to the a posteriori error analysis and continues the unifying error analysis of [18,21–23] to hanging nodes. Section 5 illustrates the abstract findings and discusses the Poisson problem, the Stokes equations, and linear elasticity. An adaptive finite element algorithm concludes the paper.

Throughout the paper, standard notation on Lebesgue and Sobolev spaces and associated norms is employed. Moreover, an inequality $A \lesssim B$ replaces $A \leq C B$ with some multiplicative mesh-size independent constant $C > 0$ that depends only on the domain Ω and the shape (e.g., through the aspect ratio) of elements ($C > 0$ is also independent of crucial parameters as the Lamè parameter λ below). Finally, $A \approx B$ abbreviates $A \lesssim B \lesssim A$.

2. 1-Irregular Triangulations

This section introduces 1-irregular triangulations as shape-1-irregular partitions with maximal one hanging node and some of their properties.

Definition 2.1 (\mathcal{T}_0) *Throughout this paper, \mathcal{T}_0 is supposed to be a regular triangulation of the 2D bounded Lipschitz domain $\Omega \subset \mathbb{R}^2$ with polygonal boundary $\partial\Omega$ into closed triangles and parallelograms. While refinements of \mathcal{T}_0 may have hanging nodes, \mathcal{T}_0 has none, i.e., two distinct elements T_1 and T_2 are either disjoint, or share exactly one vertex (called node), or share exactly one common edge.*

Definition 2.2 (Triangulations) *Throughout this paper, a triangulation \mathcal{T} is a set of triangles or parallelograms obtained by a finite number L of red-refinements from \mathcal{T}_0 , i.e., $\mathcal{T} = \mathcal{T}_L$, where for every $\ell = 1, \dots, L$ there exists one $K \in \mathcal{T}_{\ell-1}$ and \mathcal{T}_ℓ is just the former triangulation except that K is red-refined into four elements K_1, \dots, K_4 as depicted in Fig. 2.1. Then, one says that \mathcal{T} is some red-refinement of \mathcal{T}_0 .*



Fig. 2.1. Red-refinement of element domain $K = K_1 \cup K_2 \cup K_3 \cup K_4$ into 4 congruent subdomains K_1, \dots, K_4 in case of a triangle (left) and a parallelogram (right): $\text{red}(K) = \{K_1, \dots, K_4\}$.

We introduce the concept of generation of an element in a mesh. We call \mathcal{T}' a refinement of \mathcal{T} when \mathcal{T}' is constructed by replacing one or more elements $K \in \mathcal{T}$ by four sub-elements through a red-refinement bisection illustrated in Fig. 2.1 or a recursive application of this refinement. In this situation, K is called the *parent* of its four sub-elements, called *children* of K . The children of children of K are named as *grandchildren* of K .

Definition 2.3 (Generation, Node, Edge) *Given some element T of a triangulation \mathcal{T} which is some red-refinement of \mathcal{T}_0 , $|T|$ denotes its area, $\mathcal{N}(T)$ its vertices, $\mathcal{E}(T)$ its edges, and $\text{gen}(T) \in \mathbb{N}_0$ its generation provided $K \in \mathcal{T}_0$ denotes the one with $T \subseteq K$ and $\text{gen}(T) := \log |K|/|T|$. For any edge E , $\text{gen}(E)$ is similarly defined. Obviously $\text{gen}(E) = \text{gen}(K)$ provided $E \in \mathcal{E}(K)$.*

The set of nodes of the triangulation reads $\mathcal{N} := \bigcup_{T \in \mathcal{T}} \mathcal{N}(T)$, while the set of edges reads $\mathcal{E} := \bigcup_{T \in \mathcal{T}} \mathcal{E}(T)$.

Definition 2.4 (Hanging Node, k -Irregular Triangulation) *Given a triangulation \mathcal{T} which is some red-refinement of \mathcal{T}_0 , some node $z \in \mathcal{N}$ is called hanging node if some element $K \in \mathcal{T}$ satisfies*

$$z \in \partial K \setminus \mathcal{N}(K)$$

(i.e., z belongs to its boundary but is not a vertex of it). Otherwise the node $z \in \mathcal{N}$ is called regular. In case any edge $E \in \mathcal{E}$ contains at most k hanging nodes in its inside, \mathcal{T} is called k -irregular. Let \mathcal{N}_H denote the set of all hanging nodes.

Note that a 0-irregular mesh is a regular mesh (without hanging nodes) also called regular triangulation or even regular triangulation in the sense of Ciarlet [26]. In this paper, we restrict to regular and 1-irregular meshes which allow for some local mesh-refinement.

Example 2.1. Fig. 1.1 displays some mesh excluded in this paper.

Lemma 2.1. *Suppose \mathcal{T} is some 1-irregular mesh and contains two distinct T and K with intersection $E := \partial K \cap \partial T \neq \emptyset$, which includes two nodal points. Then $E \in \mathcal{E}$ is an edge and exactly one of the three cases (1), (2), (3) holds:*

1. $\text{gen}(K) = \text{gen}(T)$ and $\{E\} = \mathcal{E}(K) \cap \mathcal{E}(T)$, i.e. E is a common edge and does not contain any hanging node.
2. $\text{gen}(K) = \text{gen}(T) + 1$ and $E \in \mathcal{E}(K) \setminus \mathcal{E}(T)$, but $E \subseteq F$ for exactly one edge $F \in \mathcal{E}(T)$, which includes a hanging node $\text{mid}(F)$.
3. $\text{gen}(T) = \text{gen}(K) + 1$ and $E \in \mathcal{E}(T) \setminus \mathcal{E}(K)$, but $E \subseteq F$ for exactly one edge $F \in \mathcal{E}(K)$, which includes a hanging node $\text{mid}(F)$.

Proof. This is an immediate consequence of the definitions. □

Suppose that the closure $\overline{\Omega}$ is covered exactly by an 1-irregular triangulation \mathcal{T} of $\overline{\Omega}$ into (closed) triangles or parallelograms or mixtures of triangles and parallelograms in $2D$. It is assumed that

$$\overline{\Omega} = \cup \mathcal{T}, \quad \text{int}(K_1 \cap K_2) = 0, \quad \text{for } K_1, K_2 \in \mathcal{T}, \quad K_1 \neq K_2. \tag{2.1}$$

Here and throughout this paper, we use the concept of 1-irregular mesh from [4] with at most one hanging node on each edge.

Definition 2.5 (Hanging Edge, Child) *An edge E of an element K is called a hanging edge if its midpoint $\text{mid}(E)$ is a hanging node. The two edges E_1 and E_2 with vertex $\text{mid}(E)$ which belong to the neighbor elements K_1 and K_2 , are called children of E . Fig. 2.2 illustrates the definition of a hanging edge E and a child E_1 .*

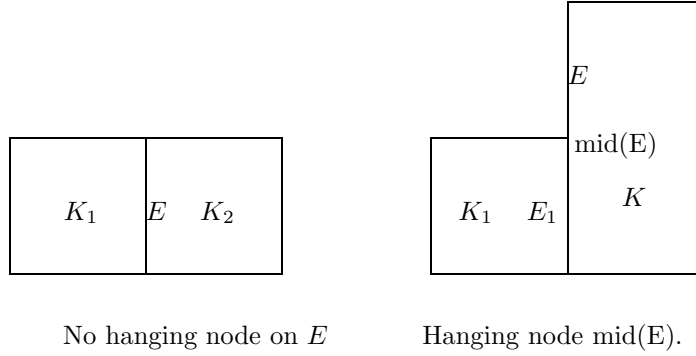


Fig. 2.2. Edges without (left) resp. with (right) hanging node.

Let \mathcal{E}_H denote the set of all hanging edges with the set of all child edges denoted by \mathcal{E}_C . The set of interior edges of Ω is denoted by $\mathcal{E}(\Omega)$. Set $\mathcal{E}_R = \mathcal{E} \setminus (\mathcal{E}_H \cup \mathcal{E}_C)$.

Let $\mathcal{N}(\omega) = \mathcal{N} \cap \bar{\omega}$ and $\mathcal{N}(\partial\Omega) = \mathcal{N} \cap \bar{\partial\Omega}$. With the set of endpoints of hanging edges \mathcal{N}_E , we set $\mathcal{N}_R = \mathcal{N} \setminus (\mathcal{N}_H \cup \mathcal{N}_E)$. By h_K and h_E we denote the diameter of the element $K \in \mathcal{T}$ and of the edge $E \in \mathcal{E}$, respectively.

For any hanging node z , we denote by $E_{1,z}$ and $E_{2,z}$ the two edges taking z as one endpoint and by E_z the hanging edge taking z as its midpoint, with $K_{1,z}$ and $K_{2,z}$ we denote the two elements such that $E_{i,z} \in \mathcal{E}(K_{i,z})$ with $i = 1, 2$, and with K_z denoted the element such that $E_z \in \mathcal{E}(K_z)$; cf. Fig. 2.3. For the triangle, we denote by $K_{3,z}$ the element with $z \in K_{3,z}$ and $E_{1,z}, E_{2,z}, E_z \notin \mathcal{E}(K_{3,z})$; cf. Fig. 2.3. For convenient notation, the index z is omitted, when there is no risk of confusion (as in Fig. 2.2).

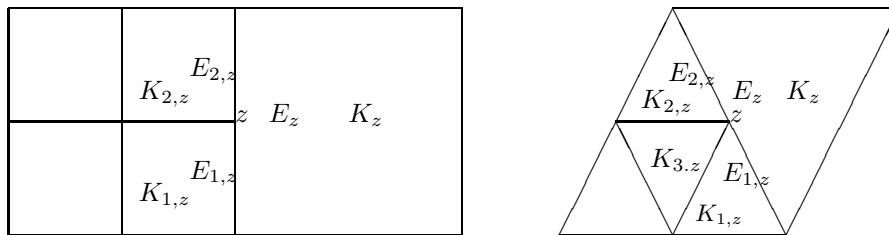


Fig. 2.3. Mesh with hanging Nodes: E_z is a hanging edge with its two children $E_{1,z}$ and $E_{2,z}$.

Let ω_K denote the union of elements $K' \in \mathcal{T}$ that share a vertex, or an edge, or a child edge of an edge with K , or share the hanging node as a vertex. Let ω_E denote the patch of elements having in common the edge E or one of the child edges of E , or share the hanging

node as a vertex. For example, $\omega_E = K_1 \cup K_2 \cup K_z$ in the left mesh depicted in Fig. 2.3, and $\omega_E = K_1 \cup K_2 \cup K_3 \cup K_z$ in the right mesh.

Given any edge $E \in \mathcal{E}$ we assign one fixed unit normal ν_E ; if (ν_1, ν_2) are its components, τ_E denotes the orthogonal vector of components $(-\nu_2, \nu_1)$. For $E \in \mathcal{E}(\partial\Omega)$ on the boundary we choose $\nu_E = \nu$, the unit outward normal to Ω , and concordantly the tangent vector τ . Once ν_E and τ_E have been fixed on E , in relation to ν_E one defines the elements $K_- \in \mathcal{T}$ and $K_+ \in \mathcal{T}$, with $E = K_+ \cap K_-$.

For the analysis, we need the following assumption on the series of meshes arising from some adaptive procedure:

(A1) Assume that the initial mesh \mathcal{T}_0 of Ω is regular in the sense of Ciarlet [13, 26], such that $\bigcup_{K \in \mathcal{T}_0} K = \bar{\Omega}$, and two distinct elements K and K' in \mathcal{T}_0 are either disjoint, or share the common edge E , or a common vertex, that is, there is no hanging node. Also, we assume that a 1-irregular mesh \mathcal{T}_{j+1} is obtained from \mathcal{T}_j by bisecting some triangles (resp. quadrilaterals) in \mathcal{T}_j into four subtriangles (resp. subquadrilaterals) through connecting their midpoints of their edges.

Remark 2.1. Fig. 1.1 shows that Assumption (A1) is necessary in some sense, otherwise one will suffer from a possible global *not*-compact support for some nodal basis.

Remark 2.2. As shown in Fig. 2.4, a strong refinement is possible in this class of meshes with 1-irregular hanging nodes.

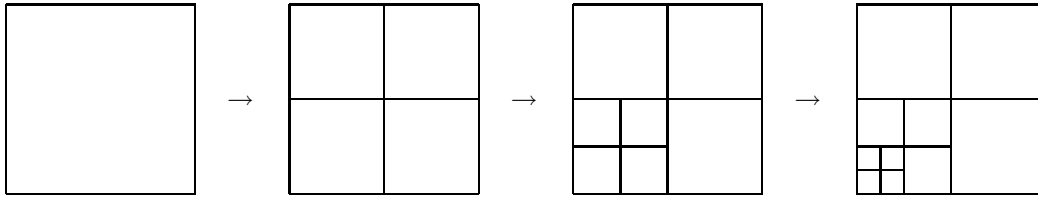


Fig. 2.4. Refinement with (A1).

Lemma 2.2. Suppose (A1) and let $|\cdot|$ denote the length of the arc. Any two distinct elements T and K with $|\partial T \cap \partial K| > 0$ satisfy that $E := \partial T \cap \partial K \in \mathcal{E}(T) \cup \mathcal{E}(K)$. If $E \in \mathcal{E}(T) \setminus \mathcal{E}(K)$ then $E \subset F \in \mathcal{E}(K)$.

Proof. The proof is immediate from (A1). □

In what follows, we give a precise description of a partition with hanging nodes of degree ≤ 1 . Given a 1-irregular mesh \mathcal{T} , we first mark some elements according to the a posteriori error estimate η with some criterion, and refine the marked elements with the red bisection, and denote the resulting mesh by $\mathcal{T}^{(0)}$. Since there may exist edges on which there are more than two hanging nodes, $\mathcal{T}^{(0)}$ may be not a 1-irregular mesh. These situations happen when one of $K_{1,z}$ and $K_{2,z}$ was refined or both of them were refined, but K_z was not refined during the aforementioned marked-refined procedure (see Fig. 2.3). Since \mathcal{T} is a 1-irregular mesh, there are at most three hanging nodes on each edge of $\mathcal{T}^{(0)}$. In what follows, we propose a closure algorithm to reduce these hanging nodes of degree = 2, 3 with the destination of a 1-irregular mesh.

Algorithm 2.1 (Compute 1-Irregular Hull) *Input:* Triangulation $\mathcal{T}^{(0)}$ with the following properties: Given some regular triangulation \mathcal{T}_0 , let the 1-irregular triangulation \mathcal{T} be obtained from \mathcal{T}_0 with a finite number of successive red-refinements. Given \mathcal{T} , red-refine some elements in \mathcal{T} to construct the input $\mathcal{T}^{(0)}$.

Loop for $\ell = 0, 1, 2, \dots$ *until termination on level* L *do*

1. Set $P_\ell := \{K \in \mathcal{T}^{(\ell)} : \exists E \in \mathcal{E}(K) \text{ such that } E \text{ contains more than one hanging node}\}$ and $M_\ell = \max\{\text{gen}(K) : K \in P_\ell\}$
2. Red-refine all elements $K \in P_\ell$ with $\text{gen}(K) = M_\ell$ to generate $\mathcal{T}^{(\ell+1)}$
3. Terminate if $\mathcal{T}^{(\ell+1)}$ is a 1-irregular triangulation and set $L := \ell + 1$ *od.*

Output: Finite number of triangulations $\mathcal{T}^{(1)}, \dots, \mathcal{T}^{(L)}$ with $M_L < \dots < M_1 < M_0$ and the 1-irregular triangulation $\mathcal{T}^{(L)}$.

Proof. Since it is the content of the termination criterion in Algorithm 2.1, obviously $\mathcal{T}^{(L)}$ is a 1-irregular triangulation. It remains to prove that the algorithm terminates in a finite number of steps. To see this, notice from the definition of M_ℓ that $0 \leq M_{\ell+1} < M_\ell$. Since $M_0 < \infty$, this implies that the algorithm has to stop in at most $M_0 + 1$ steps. \square

Lemma 2.3. *Let* z *be a new hanging node which is the midpoint of an edge* E *in a 1-irregular triangulation* \mathcal{T} *from Algorithm 2.1. Then, neither of its two endpoints* z_1 *and* z_2 *is a hanging node.*

Proof. The only non trivial case is that one of them is a hanging node in \mathcal{T} . In this case, with the refinement to create the hanging node z , there will be more than one hanging node on the edge with the midpoint z_1 resp. z_2 provided it is not bisected so far (if it is bisected, z_1 resp. z_2 is already not a hanging node). With the above algorithm, the edge(s) will be bisected to guarantee that there is only one hanging node on it, whence z_1 resp. z_2 will be not a hanging node. \square

Throughout this paper, $V := H_0^1(\Omega; \mathbb{R}^m)$ is approximated by some piecewise smooth functions.

Definition 2.6 (Broken Sobolev Spaces) *Given any triangulation* \mathcal{T} , *set*

$$H^1(\mathcal{T}) = \{v \in L^2(\Omega) : \forall K \in \mathcal{T}, v|_K \in H^1(K)\}.$$

For any $v \in H^1(\mathcal{T})$, *let* $\nabla_h v$ *be the piecewise gradient operator (piecewise with respect to* \mathcal{T} *),* $\nabla_h v|_K := \nabla(v|_K)$. *Moreover, let* $[v]_E = v|_{K_+} - v|_{K_-}$ *denote the jump of* $v \in H^1(\mathcal{T})$ *across the edge* $E = K_+ \cap K_-$.

Definition 2.7 (Finite Element Spaces) *For a non-negative integer* k , $Q_k(\omega)$ *denotes the polynomial space of total degree* $\leq k$ *for triangular elements and degree* $\leq k$ *in each variable for quadrilateral elements. For this presentation it will suffice to assume* $k = 1$. *The corresponding conforming space will be denoted by*

$$V_h^C := \{v \in V : \forall K \in \mathcal{T}, v|_K \in Q_1(K; \mathbb{R}^m)\}$$

Theorem 2.1 (Approximation and Stability) *Given the finite element space $V_h^C \subset V := H_0^1(\Omega; \mathbb{R}^m)$ based on an aforementioned 1-irregular triangulation \mathcal{T} there exists an approximation operator $\mathcal{J} : V \rightarrow V_h^C$ such that, for all $v \in V$,*

$$\|\nabla \mathcal{J}v\|_{L^2(\Omega)}^2 + \sum_{T \in \mathcal{T}} h_T^{-2} \|(v - \mathcal{J}v)\|_{L^2(T)}^2 + \sum_{E \in \mathcal{E}} h_E^{-1} \|(v - \mathcal{J}v)\|_{L^2(E)}^2 \lesssim \|\nabla v\|_{L^2(\Omega)}.$$

Proof. The nodal basis of the space V_h^C is described in the sequel. For any $z \in \mathcal{N}_R$ the nodal basis function φ_z is defined in a usual way by $\varphi_z \in Q_1(K)$ for any $K \in \mathcal{T}$ with $\varphi_z(z) = 1$ and $\varphi_z(P) = 0$ for all $P \in \mathcal{N} \setminus \{z\}$. We define the nodal function for any node $z \in \mathcal{N}_H$ by $\varphi_z \in Q_1(K_{i,z})$, $i = 1, \dots, \ell$ with $\ell = 2$ for the quadrilateral mesh and $\ell = 3$ for the triangle mesh, $\varphi_z(z) = 1$, and $\varphi_z(P) = 0$ for all $P \in \mathcal{N}(K_{1,z} \cup \dots \cup K_{\ell,z}) \setminus \{z\}$, and $\varphi_z(x) = 0$ for all $x \in \overline{\Omega} \setminus (\overline{K_{1,z}} \cup \dots \cup \overline{K_{\ell,z}})$. To define the nodal basis function for node $z \in \mathcal{N}_E$, we first define

$$\varphi'_z|_K = \varphi_K \text{ for any } K \in \mathcal{T}(z). \quad (2.2)$$

Here, $\mathcal{T}(z)$ denotes the set of elements having the vertex z , and φ_K is defined as

$$\varphi_K(z) = 1, \quad \varphi_K(P) = 0 \quad \text{for all } P \in \mathcal{N}(K) \setminus \{z\}, \quad \varphi_K \in Q_1(K). \quad (2.3)$$

Denote by $\mathcal{E}_{H,z}$ the set of hanging edges taking node z as one of its endpoints with $\mathcal{N}_{H,z}$ the set of midpoints. Then the nodal basis function for any node $z \in \mathcal{N}_E$ can be defined as

$$\varphi_z = \varphi'_z + \frac{1}{2} \sum_{P \in \mathcal{N}_{H,z}} \varphi_P \in V_h^C := \text{span}\{\varphi_z : z \in (\mathcal{N}_E \cup \mathcal{N}_R) \setminus \mathcal{N}(\partial\Omega)\}. \quad (2.4)$$

Notice that $(\varphi_z : z \in \mathcal{N}_E \cup \mathcal{N}_R)$ forms a partition of unity. With this partition of unity, one can define the Clément interpolation operator [17] (or any other regularized conforming finite element approximation operator) $\mathcal{J} : H_0^1(\Omega) \mapsto V_h^C$ with

$$\|\nabla \mathcal{J}\varphi\|_{L^2(K)} + \|h_K^{-1}(\varphi - \mathcal{J}\varphi)\|_{L^2(K)} \lesssim \|\nabla \varphi\|_{L^2(\omega_K)}, \quad (2.5)$$

$$\|h_E^{-1/2}(\varphi - \mathcal{J}\varphi)\|_{L^2(E)} \lesssim \|\nabla \varphi\|_{L^2(\omega_E)}, \quad (2.6)$$

for all $K \in \mathcal{T}$, $E \in \mathcal{E}_R \cup \mathcal{E}_H$, and $\varphi \in H_0^1(\Omega)$.

Based on the basis functions $\{\varphi_z : z \in \mathcal{N}_E \cup \mathcal{N}_R\}$, one can construct [17] a Lipschitz continuous partition of unity

$$\{\psi_z : z \in \mathcal{N}_E \cup \mathcal{N}_R\} \quad (\text{Lipschitz partition of unity}) \quad (2.7)$$

with

$$\sum_{z \in \mathcal{K}} \psi_z = 1 \text{ in } \Omega, \quad \mathcal{K} = \mathcal{N}_R \cup \mathcal{N}_E \setminus \partial\Omega. \quad (2.8)$$

Moreover, for any $z \in \mathcal{K}$, suppose that ψ_z vanishes outside an open and connected set $\Omega_z \subseteq \Omega$

$$\text{supp}\psi_z \subseteq \overline{\Omega}_z, \quad \max_{x \in \overline{\Omega}} \text{card}\{z \in \mathcal{K} : x \in \Omega_z\} \lesssim 1. \quad (2.9)$$

Given $z \in \mathcal{K}$, let $\mathcal{E}(z) := \{E \in \mathcal{E}_R \cup \mathcal{E}_H : \psi_z|_E \neq 0\}$ denote the set of edges, where ψ_z is nonvanishing. For any edge E let $\mathcal{K}(E)$ denote the set of all $z \in \mathcal{K}$ with $E \in \mathcal{E}(z)$.

The finite overlap and the summation of (2.5)-(2.6) lead to the assertion. \square

3. A Priori Error Analysis

This section is devoted to the a priori error analysis of a mixed formulation which covers applications of Section 5 and which provides the setting for a unified a posteriori error analysis of Section 4. Throughout this paper, we will consider some Lebesgue space Q and some Sobolev space V and bounded bilinear forms

$$a : V \times V \rightarrow \mathbb{R}, \quad b : Q \times V \rightarrow \mathbb{R}, \quad c : Q \times Q \rightarrow \mathbb{R}. \quad (3.1)$$

Suppose a , b , and c satisfy

$$\|v\|_V^2 \lesssim a(v, v) \quad \forall v \in V, \quad (3.2)$$

$$\|q\|_Q \lesssim \sup_{v \in V \setminus \{0\}} \frac{b(q, v)}{\|v\|_V}, \quad (3.3)$$

$$0 \leq c(q, q) \lesssim \|q\|_Q^2 \quad \forall q \in Q. \quad (3.4)$$

Then, the exact problem has a unique solution [11, 15] in the sense that, given right-hand side $g \in V^*$, there exists some unique $(u, p) \in V \times Q := H_0^1(\Omega)^m \times L_0^2(\Omega)$ with

$$a(u, v) + b(p, v) = g(v) \quad \forall v \in V, \quad (3.5)$$

$$b(q, u) - t^2 c(p, q) = 0 \quad \forall q \in Q. \quad (3.6)$$

The well-posedness of (3.5)-(3.6) is t -independent, in the sense that the norm of the inverse operator does not depend on t . Define the following norm

$$\| \! \| (v, q) \! \| \! \| ^2 := a(v, v) + \|q\|_Q^2 + t^2 c(q, q) \quad \text{for any } v \in V, \quad q \in Q. \quad (3.7)$$

Let $Q_h \subset Q$ and $V_h + V \subset H^1(\mathcal{T}; \mathbb{R}^m)$ be some (conforming and nonconforming) discrete spaces associated to some 1-irregular triangulation \mathcal{T} . It is assumed that integral means of jumps of discrete functions vanish:

(A2) For all $v_h \in V_h$ it holds

$$\int_E [v_h] ds = 0, \quad E \in \mathcal{E}_R \cup \mathcal{E}_H. \quad (3.8)$$

Moreover, let $a_h : (V + V_h) \times (V + V_h) \rightarrow \mathbb{R}$ and $b_h : Q \times (V + V_h) \rightarrow \mathbb{R}$ be some extensions of a and b in the sense that $a_h|_{V \times V} = a$ and $b_h|_{Q \times V} = b$.

(A3) There exists a (Fortin interpolation) operator $\Pi_F : V \rightarrow V_h$ with

$$b_h(q, v - \Pi_F v) = 0 \quad \forall q \in Q_h, \quad \|\Pi_F v\|_h \lesssim \|v\|_V \quad \forall v \in V. \quad (3.9)$$

Given $g_h \in V_h^*$, let (u_h, p_h) be the unique solution of the discrete problem

$$a_h(u_h, v_h) + b_h(p_h, v_h) = g_h(v_h) \quad \forall v_h \in V_h, \quad (3.10)$$

$$b_h(q_h, u_h) - t^2 c(q_h, p_h) = 0 \quad \forall q_h \in Q_h. \quad (3.11)$$

The associated discrete norms read, for all $v \in V + V_h$ and $q \in Q$,

$$\|v\|_h^2 := a_h(v, v), \quad \| \! \| (v, q) \! \| \! \| _h^2 := \|v\|_h^2 + \|q\|_Q^2 + t^2 c(q, q). \quad (3.12)$$

Let Du denote the functional matrix of all first-order partial derivatives (e.g., the gradient and possibly also the Green strain of linear elasticity) of the Sobolev function u with D_h the piecewise counterpart of the operator D .

Theorem 3.1 (A Priori Error Estimates) *Let $(u, p) \in V \times Q$ and $(u_h, p_h) \in V_h \times Q_h$ solve the Problem (3.5)-(3.6) and Problem (3.10)-(3.11), respectively. Assume that the spaces Q_h and V_h satisfy (A2)-(A3). (a) It holds*

$$\begin{aligned} \|(u - u_h, p - p_h)\|_h &\lesssim \inf_{(v_h, q_h) \in V_h \times Q_h} \|(u - v_h, p - q_h)\|_h \\ &\quad + \sup_{w_h \in V_h \setminus \{0\}} \frac{a_h(u, w_h) + b_h(p, w_h) - g_h(w_h)}{\|w_h\|_h}. \end{aligned}$$

(b) *Suppose that there exists some $\sigma \in H^1(\Omega; \mathbb{R}^{m \times n})$ such that $g_h \in V_h^*$ and $(u, p) \in V \times Q$ satisfy, for all $v_h \in V_h$,*

$$g_h(v_h) = - \int_{\Omega} v_h \cdot \operatorname{div} w \sigma \, dx, \quad a_h(u, v_h) + b_h(p, v_h) = \int_{\Omega} \sigma : D_h v_h \, dx. \quad (3.13)$$

Let $h_{\mathcal{T}}$ denote the piecewise constant local mesh-size, i.e., $h_{\mathcal{T}}|_K = h_K$ for all $K \in \mathcal{T}$. Then it holds

$$\sup_{w_h \in V_h \setminus \{0\}} \frac{a_h(u, w_h) + b_h(p, w_h) - g_h(w_h)}{\|D_h w_h\|_{L^2(\Omega)}} \lesssim \|h_{\mathcal{T}} D \sigma\|_{L^2(\Omega)}.$$

Remark 3.1. The characterisation of σ in (3.13) reflects consistency of the continuous solution (u, p) in the discrete situation with exact integration of the right-hand sides and then controls the inconsistency error in (b).

Proof. For any $(v_h, q_h) \in V_h \times Q_h$, the Fortin interpolation operator from Assumption (A3) yields the discrete inf-sup condition (cf., e.g., [10, Theorem 1] for a proof). That guarantees the existence of $(w_h, r_h) \in V_h \times Q_h$ with norm $\|(w_h, r_h)\|_h \approx 1$ and

$$\begin{aligned} &\|(u_h - v_h, p_h - q_h)\|_h \\ &\lesssim a_h(u_h - v_h, w_h) + b_h(r_h, u_h - v_h) + b_h(p_h - q_h, w_h) - t^2 c(r_h, p_h - q_h). \end{aligned}$$

This and standard manipulations with the discrete and exact equations show

$$\begin{aligned} &\|(u_h - v_h, p_h - q_h)\|_h \\ &\lesssim a_h(u_h - u, w_h) + b_h(r_h, u_h - u) + b_h(p_h - p, w_h) - t^2 c(r_h, p_h - p) \\ &\quad + a_h(u - v_h, w_h) + b_h(r_h, u - v_h) + b_h(p - q_h, w_h) - t^2 c(r_h, p - q_h) \\ &\lesssim \|(u - v_h, p - q_h)\|_h - a_h(u, w_h) - b_h(p, w_h) + g_h(w_h). \end{aligned}$$

Together with a triangle inequality, this proves (a).

The extra conditions in (b) on the field σ allow for, for any $w_h \in V_h$,

$$a_h(u, w_h) + b_h(p, w_h) - g_h(w_h) = \int_{\Omega} (w_h \cdot \operatorname{div} w \sigma + \sigma : D_h w_h) \, dx.$$

An elementwise integration by parts with the Sobolev function σ and the \mathcal{T} -piecewise smooth function w_h result in a cancelation of the element volume contributions and remaining jump terms along the edges. In fact,

$$a_h(u, w_h) + b_h(p, w_h) - g_h(w_h) = \sum_{E \in \mathcal{E}_H \cup \mathcal{E}_R} \int_E (\sigma \nu_E)[w_h] \, ds.$$

For any $E \in \mathcal{E}_R$, $\int_E [w_h] ds = 0$ by (A2). This allows for

$$\int_E (\sigma \nu_E) [w_h] ds = \int_E ((\sigma - \bar{\sigma}) \nu_E) [w_h] ds$$

for some integral mean $\bar{\sigma} \in \mathbb{R}^{m \times n}$. A standard trace inequality followed by a Poincaré inequality leads to

$$\int_E (\sigma \nu_E) [w_h] ds \lesssim h_E^{1/2} \|D\sigma\|_{L^2(\omega_E)} \| [w_h] \|_{L^2(E)}. \quad (3.14)$$

Similar arguments for the jump term of $w_h - \bar{w}_h$ on the patch ω_E yield

$$\int_E (\sigma \nu_E) [w_h] ds \lesssim h_E \|D\sigma\|_{L^2(\omega_E)} \|D_h w_h\|_{L^2(\omega_E)}. \quad (3.15)$$

To analyse the second case, let z be the hanging node on $E = E_1 + E_2 \in \mathcal{E}_H$ and let $\pi_0^E v = \frac{1}{h_E} \int_E v ds$ denote the integral mean along E . Let $K_{j,z}$ be some element domain with vertex z and edge E_j for $j = 1, 2$ and let $w_h|_{K_{1,z} \cup \dots \cup K_{\ell,z}}$ denote the restriction of w_h to the one-sided neighborhood $K_{1,z} \cup \dots \cup K_{\ell,z} \subset \omega_E$ of E with integral mean $\pi_0^E w|_{K_{1,z} \cup \dots \cup K_{\ell,z}}$ along E . The estimate

$$\|w_h|_{K_{1,z} \cup \dots \cup K_{\ell,z}} - \pi_0^E w_h|_{K_{1,z} \cup \dots \cup K_{\ell,z}}\|_{L^2(E)} \lesssim h_E^{1/2} \|\nabla_h w_h\|_{L^2(K_{1,z} \cup \dots \cup K_{\ell,z})} \quad (3.16)$$

again follows from standard arguments on piecewise trace inequalities and elementwise Poincaré inequalities. Let K denote the element domain with edge E opposite of $K_{1,z} \cup \dots \cup K_{\ell,z}$. Then, as in (3.16), one deduces

$$\|w_h|_K - \pi_0^E w_h|_K\|_{L^2(E)} \lesssim h_E^{1/2} \|\nabla_h w_h\|_{L^2(K)}. \quad (3.17)$$

The above arguments from the first case allow for (3.14), (3.16) and (3.17) yield (3.15) in the second case as well. Since the edge patches have finite overlap, the aforementioned inequalities (3.14) result in

$$\sum_{E \in \mathcal{E}_R \cup \mathcal{E}_H} \int_E (\sigma \nu_E) [w_h] ds \lesssim \|h_T D\sigma\|_{L^2(\Omega)} \|D_h w_h\|_{L^2(\Omega)}. \quad \square$$

4. A Posteriori Error Analysis

This section is devoted to the a posteriori error analysis of the methods of the previous section and adopts its notation. The unified theory of a posteriori error analysis [18, 20, 22, 23] considers the operator $A : V \times Q \rightarrow V^* \times Q^*$ with $V = H_0^1(\Omega; \mathbb{R}^m)$ and $Q = L^2(\Omega; \mathbb{R}^{m \times n})$ and

$$(A(p, u))(q, v) := a(u, v) + b(p, v) + b(q, u) - t^2 c(p, q) \quad (4.1)$$

for all $(u, p), (q, v) \in V \times Q$. Then the continuous problem (3.5)-(3.6) is equivalent to

$$(A(p, u))(q, v) := a(u, v) + b(p, v) + b(q, u) - t^2 c(p, q) = g(v). \quad (4.2)$$

The norm in Q is defined as in [25, 33] by

$$\|q\|_Q = \sup_{v \in V \setminus \{0\}} \frac{b(q, v)}{\|v\|_V} + t \sqrt{c(q, q)}, \quad \forall q \in Q. \quad (4.3)$$

It follows from (3.3) that

$$\|q\|_Q \approx \|q\|_Q \quad \text{uniformly with respect to } 0 \leq t \leq 1. \quad (4.4)$$

The condition (3.2) and the general theory of mixed finite element formulations [10, Theorem 2] show that the bilinear form A is an isomorphism between $V \times Q$ and its dual. This means

$$\|(u, p)\| \approx \sup_{(v, q) \in V \times Q \setminus \{(0,0)\}} \frac{(A(p, u))(q, v)}{\|(v, q)\|}. \quad (4.5)$$

Suppose $(\tilde{u}_h, p_h) \in V \times Q$ is some approximation to the exact solution (u, p) and define the residuals

$$\mathcal{R}es_V(v) := g(v) - a(\tilde{u}_h, v) - b(p_h, v), \quad \forall v \in V, \quad (4.6)$$

$$\mathcal{R}es_Q(q) := b(q, \tilde{u}_h) - t^2 c(p_h, q), \quad \forall q \in Q. \quad (4.7)$$

Here and throughout, \tilde{u}_h belongs to V and denotes some continuous and *not* necessarily discrete function; however, the subindex in \tilde{u}_h refers to the fact that \tilde{u}_h might be closely related (or designed with some post-processing) to some discrete function u_h (which, typically, does not belong to V for nonconforming finite element methods). Below we choose \tilde{u}_h as some best approximation to u_h in V in the sense of

$$\|u_h - \tilde{u}_h\|_h \approx \min_{v \in V} \|u_h - v\|_h.$$

For all applications we have in mind, the minimum can be controlled with the help of the Lipschitz partition of unity (2.7) and one fundamental result from [22, Theorem 3.1],

$$\min_{\tilde{u}_h \in V} \|D_{\mathcal{T}} u_h - D \tilde{u}_h\|_{L^2(\Omega)}^2 \lesssim \mu^2 := \sum_{E \in \mathcal{E}} \sum_{z \in \mathcal{K}(E)} h_E \|\tau_E \cdot [D_h(\psi_z u_h)]\|_{L^2(E)}^2. \quad (4.8)$$

Notice that here the boundary edges are included in \mathcal{E} which, indeed, clarifies the notational gap of [22]; τ_E denote the tangential vectors and (4.8) holds without any further assumption on the piecewise gradient of u_h .

Coming back to the abstract situation and \tilde{u}_h in V , it holds

$$\|(u - \tilde{u}_h, p - p_h)\| \approx \|\mathcal{R}es_V\|_{V^*} + \|\mathcal{R}es_Q\|_{Q^*} \quad (4.9)$$

and it remains to estimate the residuals.

Recall that $(u, p) \in V \times Q$ solves (3.5)-(3.6) and $(u_h, p_h) \in V_h \times Q_h$ solves (3.10)-(3.11).

Assume that Q_h and V_h satisfy (A2)-(A3) plus a further assumption (A4) and (A5) from [22, 23] which involves the existence of σ_h and an interpolation operator Π_h as follows:

(A4) There exists some $\sigma_h \in H^1(\mathcal{T}; \mathbb{R}^{m \times n})$ which satisfies

$$a_h(u_h, v_h) + b_h(p_h, v_h) = \int_{\Omega} \sigma_h : D_h v_h \, dx, \quad \forall v \in V + V_h.$$

(A5) There exists some bounded, linear operator $\Pi_h : V_h^C \rightarrow V_h$ with the properties (4.10)-(4.11) for every $v_h \in V_h^C$ and all $K \in \mathcal{T}$,

$$\int_{\Omega} \sigma_h : D_h(v_h - \Pi_h v_h) \, dx = 0, \quad \int_K (v_h - \Pi_h v_h) \, dx = 0, \quad (4.10)$$

$$\|D\Pi_h v_h\|_{L^2(K)} \lesssim \|Dv_h\|_{L^2(\omega_K)}. \quad (4.11)$$

For some given $f \in L^2(\Omega)$, let $g_h \in V_h^*$ be defined by

$$g(v) = g_h(v) := \int_{\Omega} f v \, dx, \quad \forall v \in V.$$

For f and its piecewise constant approximation f_h with respect to \mathcal{T} , we refer to $\text{osc}(f)$ as oscillation of f [40],

$$\text{osc}^2(f) := \sum_{K \in \mathcal{T}} h_K^2 \|f - f_h\|_{L^2(K)}^2. \quad (4.12)$$

The piecewise smooth σ_h from (A4) defines jumps $[\sigma_h]_E$ of the discontinuous discrete stress across an interior edge E with unit normal ν_E ,

$$[\sigma_h]_E(x) = (\sigma_h|_{K_+}(x) - \sigma_h|_{K_-}(x)), \quad x \in E = K_- \cap K_+.$$

Then, the residual-based a posteriori error estimator reads

$$\eta^2 := \sum_{K \in \mathcal{T}} h_K^2 \|g + \text{div} w \sigma_h\|_{L^2(K)}^2 + \sum_{E \in \mathcal{E}(\Omega) \cap (\mathcal{E}_R \cup \mathcal{E}_H)} h_E \|[\sigma_h]_E \cdot \nu_E\|_{L^2(E)}^2. \quad (4.13)$$

Since the norm in Q is some Lebesgue norm, the dual norm

$$\xi := \|b_h(\cdot, u_h) - t^2 c(\cdot, p_h)\|_{Q^*}$$

can be estimated easily.

Theorem 4.1 (A Posteriori Error Estimates) *For (A1)-(A5) holds*

$$\|(u - \tilde{u}_h, p - p_h)\| \lesssim \eta + \|u_h - \tilde{u}_h\|_h + \xi + \text{osc}(f). \quad (4.14)$$

Proof. Given $v \in V \setminus \{0\}$, set $v_h^C = \mathcal{J}v$ as in Theorem 2.1 and set $v_h^{NC} := \Pi_h v_h^C$. Then (A4) yields

$$\mathcal{R}es_V(v) := g(v) - a(\tilde{u}_h, v) - b_h(p_h, v) = a(u_h - \tilde{u}_h, v) + \int_{\Omega} (f \cdot v - \sigma_h : Dv) \, dx.$$

The right-hand side g equals g_h and hence the discrete equation shows

$$0 = \int_{\Omega} (f \cdot v_h^{NC} - \sigma_h : Dv_h^{NC}) \, dx.$$

With (A5) follows

$$\int_{\Omega} (f \cdot v_h^C - \sigma_h : Dv_h^C) dx = \int_{\Omega} f \cdot (v_h^C - \Pi_h v_h^C) dx$$

and $v_h^C - \Pi_h v_h^C$ has piecewise integral means zero, e.g.,

$$\int_{\Omega} f_h \cdot (v_h^C - \Pi_h v_h^C) dx = 0.$$

This and an elementwise Poincaré inequality show

$$\left| \int_{\Omega} (f \cdot v_h^C - \sigma_h : Dv_h^C) dx \right| \lesssim \text{osc}(f) \|D_h(v_h^C - \Pi_h v_h^C)\|_{L^2(\Omega)}.$$

Consequently, with $w := v - v_h^C$,

$$\mathcal{R}es_V(v) \lesssim a(u_h - \tilde{u}_h, v) + \int_{\Omega} (f \cdot w - \sigma_h : Dw) dx + \text{osc}(f) \|D_h(v_h^C - \Pi_h v_h^C)\|_{L^2(\Omega)}.$$

The stability of operators \mathcal{J} and Π_h plus the boundedness of a yields

$$\mathcal{R}es_V(v) / \|v\|_V \lesssim \|u_h - \tilde{u}_h\|_V + \int_{\Omega} (f \cdot w - \sigma_h : Dw) dx / \|w\| + \text{osc}(f).$$

The estimation of

$$\int_{\Omega} (f \cdot w - \sigma_h : Dw) dx \lesssim \|w\| \eta$$

is well-established and may follow [1, 7, 18, 40]. The second residual is obviously bounded by its norm ξ . □

5. Applications

This section applies the theory from the previous sections to three problems, i.e., the Poisson problem, the Stokes problem, and the linear elasticity problem. We shall briefly give some examples with Assumptions (A2)-(A5).

5.1. Remarks on the Poisson Equation

Given the right-hand side $f \in L^2(\Omega)$, seek $u \in V := H_0^1(\Omega)$ with

$$-\Delta u = f \in V^* \equiv H^{-1}(\Omega).$$

The abstract framework covers the weak form with the bilinear forms a and a_h ,

$$a_h(u, v) := \int_{\Omega} \nabla_h u : \nabla_h v dx, \text{ for any } u, v \in H^1(\mathcal{T}), \tag{5.1}$$

and $m = 1$, $b \equiv 0$, and $t = 0$. Moreover, $\sigma := \nabla u$ and $\sigma_h := \nabla_h u_h$.

Since (3.3) is violated, the a priori and a posteriori error analysis of Sections 3 and 4 is not applicable. However, the above arguments on $a := a_h|_{V \times V}$ and a_h are applicable and prove the standard estimates of the unifying theory [18, 20, 22] for triangulations with hanging nodes.

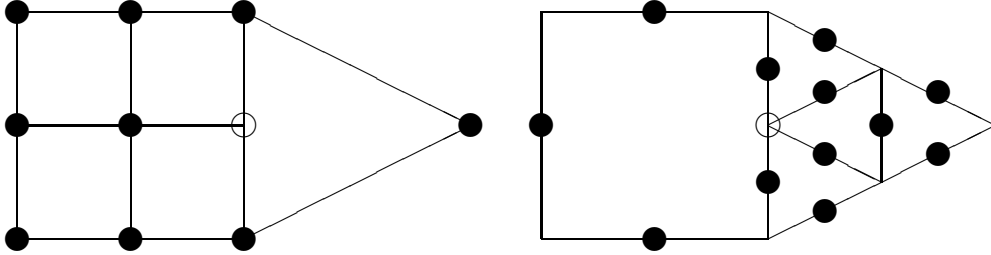


Fig. 5.1. Triangulation with conforming (left) and nonconforming (right) P_1 and Q_1 elements and one hanging edge $E_H = E_{H,1} \cup E_{H,2}$.

For this problem, these assumptions (A2)-(A5) are satisfied by the Courant element, the bilinear Q_1 element, the Crouzeix-Raviart element [27], the Han element [32], the nonconforming rotated Q_1 element [37], the constrained nonconforming rotated Q_1 element [34], the DSSY [30]; the justification immediately follows from the definitions of these elements and the arguments of [22, 23]. These elements are illustrated in Table 1.1.

Let us briefly comment on the underlying assumptions (A1)-(A5) of which only the last one may be seen as questionable. We illustrate the fact that the arguments of [22, 23] validate (A5) on the simplest relevant example of nonconforming rotated Q_1 element after Rannacher and Turek [37] combined with some nonconforming P_1 element after Crouzeix-Raviart [27].

Given any continuous and piecewise P_1 or Q_1 function v_h^C on the left mesh of Fig. 5.1, the interpolant $v_h^{NC} := \Pi_h v_h^C \in V_h$ in the nonconforming finite element space associated to the right mesh is defined through the integral of each edge E of some element domain K . In other words,

$$\int_E (v_h^C - v_h^{NC}|_K) ds = 0,$$

for all edges E and neighbouring K . This definition applies to E_H and $E_{H,j}$ of Fig. 5.1 as well and then implies (A2). The verification of (A5) is a local argument: An integration by parts on any K proves (where $\mathcal{E}(K)$ denotes the set of edges of K)

$$\int_K D(v_h^C - v_h^{NC}) dx = \int_{\partial K} (v_h^C - v_h^{NC}) \nu_T ds = \sum_{E \in \mathcal{E}(K)} \pm \nu_E \int_E (v_h^C - v_h^{NC}) ds = 0.$$

Here we did not care about the orientation of ν_T along the edges and wrote $\pm \nu_E$ knowing that it is, by design of v_h^C , multiplied by zero anyway. In cases where $\sigma_h = D_h u_h$ is constant on K , this proves the first part of (4.10). The only nonconstant case is studied on the reference element $K = Q_{\text{ref}} = (-1, 1)^2$ where, as a typical model case,

$$u_h(\xi, \eta) := (\xi^2 - \eta^2)/2$$

and hence $\sigma_h(\xi, \eta) = (\xi, -\eta)$. Then, $\text{div} w \sigma_h$ vanishes and, moreover, $\sigma_h \cdot \nu_E$ is constant for any edge $E \in \mathcal{E}(Q_{\text{ref}})$. Therefore, for this model case, the integration by parts argument shows the first part of (4.10) on K as well.

The remaining hypothesis of the second part of (4.10) follows for affine functions and appears

crucial only for the model situation where, again on $K = Q_{\text{ref}}$,

$$v_h^C(\xi, \eta) = (1 + \xi)(1 + \eta)$$

and so $v_h^{NC}(\xi, \eta) = 1 + \xi + \eta$ is in fact affine. A direct calculation shows the second part of (4.10) for this particular case. The general situation follows immediately by symmetry and combination of it.

The moral of the example analysis is that the edge-oriented definition of the operator Π_h in the previous papers [22, 23] remains valid because it is an elementwise design. Therefore, the assumption (A5) follows in all cases as well and we leave out the details here: There is no change of arguments in the situation with hanging nodes.

The error estimators are essentially the ones from the literature with small modifications in the weight functions which are the nodal basis functions in V_h^C for 1-irregular triangulations of Section 2. Therefore, more details are omitted.

5.2. The Stokes Problem

In the well-established weak form of the Stokes problem [11, 13, 15, 31], the bilinear forms $a := a_h|_{V \times V}$ and a_h read

$$a(u, v) = \mu \int_{\Omega} D_h u : D_h v \, dx \text{ for the unsymmetric formulation,}$$

$$a(u, v) = \mu \int_{\Omega} \varepsilon_h(u) : \varepsilon_h(v) \, dx \text{ for the symmetric formulation,}$$

for all $u, v \in H^1(\mathcal{T}; \mathbb{R}^n)$, $m = n$, with the (piecewise) symmetric gradient

$$\varepsilon_h(u) = \frac{1}{2}(D_h u + D_h u^T).$$

Moreover,

$$Q = L^2(\Omega)/\mathbb{R} = \left\{ q \in L^2(\Omega) : \int_{\Omega} q \, dx = 0 \right\}$$

and, for all $q \in L^2(\Omega)$ and $v \in H^1(\mathcal{T}; \mathbb{R}^n)$,

$$b(q, u) = \int_{\Omega} q \operatorname{div} w_h u \, dx, \quad c \equiv 0, \quad t = 0.$$

For this problem, Assumptions (A2)-(A5) are satisfied by all examples listed in Table 1.2 and analyzed in [22] except the Hu-Man-Shi element. The stress fields read

$$\sigma = \mu D u - p \mathbf{I}, \quad \sigma_h = \mu D_h u_h - p_h \mathbf{I} \text{ for the unsymmetric formulation,}$$

$$\sigma = \mu \varepsilon u - p \mathbf{I}, \quad \sigma_h = \mu \varepsilon_h u_h - p_h \mathbf{I} \text{ for the symmetric formulation,}$$

Notice that

$$\xi = \|\operatorname{div} w \sigma_h\|_{L^2(\Omega)}$$

monitors the incompressibility constraints in the discrete situation [18, 22, 24, 28].

Remark 5.1. Since (A3) does not hold for the Hu-Man-Shi element, the a priori analysis herein is inapplicable for it. However the a posteriori analysis of this paper equally holds for it.

5.3. Linear Elasticity

The linear elastic problem encounters the locking phenomenon as the Lamé parameter λ becomes larger and larger in an incompressible limit scenario. One particular model of this yields a weak formulation with a pressure variable p and, in fact, leads to the weak formulation (3.5)-(3.6) with a , a_h , b , and b_h as in the previous subsection and the bilinear form $c : Q \times Q \rightarrow \mathbb{R}$ defined by

$$c(p, q) = \int_{\Omega} p q \, dx, \quad t^2 = \frac{1}{\lambda}.$$

Then, with the stress fields σ and σ_h as above, all assumptions (A2)-(A5) are satisfied by all examples analyzed in [22] except the Hu-Man-Shi element.

With some projection operator Π_2 from the context of the locking (see [22] for details), it holds

$$\xi = \|\Pi_2 \operatorname{div} w_h u_h - \operatorname{div} w_h u_h\|_{L^2(\Omega)}.$$

5.4. Adaptive finite element method

An element-oriented adaptive mesh-refining algorithm is described in this subsection with 1-irregular triangulations \mathcal{T} generated by Algorithm 5.1.

Algorithm 5.1. *Input: Coarse regular triangulation \mathcal{T}_0 with rectangular and/or triangular elements.*

Loop for $\ell = 0, 1, 2, \dots$ until termination on level L do

1. *Solve discrete problem on \mathcal{T}_ℓ with N degrees of freedom.*
2. *For all $K \in \mathcal{T}_\ell$ compute*

$$\eta_K^2 := h_K^2 \|f + \operatorname{div} w \nabla u_h\|_{L^2(K)}^2 + \frac{1}{2} \sum_{E \in \mathcal{E}(K)} h_E \|[\partial_h u_h]\|_{L^2(E)}^2.$$

and set $\eta_N := (\sum_{K \in \mathcal{T}} \eta_K^2)^{1/2}$.

3. *Mark $K \in \mathcal{M} \subset \mathcal{T}_\ell$ for refinement into four congruent elements by connecting the midside points of its edges provided $\theta \max_{T \in \mathcal{T}_\ell} \eta_T \leq \eta_K$.*
4. *Run Algorithm 2.1 with input $\operatorname{red}(\mathcal{M}) \cup (\mathcal{T}_\ell \setminus \mathcal{M})$ and output $\mathcal{T}_{\ell+1}$ od.*

Output: Sequence of triangulations $\mathcal{T}_1, \dots, \mathcal{T}_L$ and discrete solutions plus error estimators η_N .

5.5. Numerical example

In [23], Algorithm 5.1 was run for the NR element from [37] to approximate the Dirichlet problem with $g \equiv 0$ and smooth Dirichlet data u_D on the L-shaped domain with exact solution (written in polar coordinates)

$$u(r, \theta) = r^{2/3} \sin\left(\frac{2}{3}\theta\right).$$

The adaptive algorithm of the previous subsection involves approximation error terms on the Dirichlet data in the tangential jump and generates a sequence of meshes displayed in Fig. 5.2 with a local refinement towards the reentrant corner with Fig. 5.3 displays experimental convergence rates for the exact error and the estimate η_N .

Fig. 5.3 displays experimental convergence rates for the exact error and the estimate η_N for uniform and adaptive refinement with the corresponding triangulations depicted in Fig. 5.2.

The adaptive refinement improves the convergence rate of uniform refinement to the optimal one $\theta(N^{-1/2})$ with respect to the number N of degrees of freedom, and the convergence rate of the estimate mirrors the one of the exact error both for uniform and adaptive refinement. A more detailed analysis on the numbers shows that

$$2.13 \leq \eta_N / \|\nabla_h e_N\| \leq 2.83$$

for adaptive and

$$2.13 \leq \eta_N / \|\nabla_h e_N\| \leq 2.35$$

for uniform mesh refinement. This confirms the theoretical predictions.

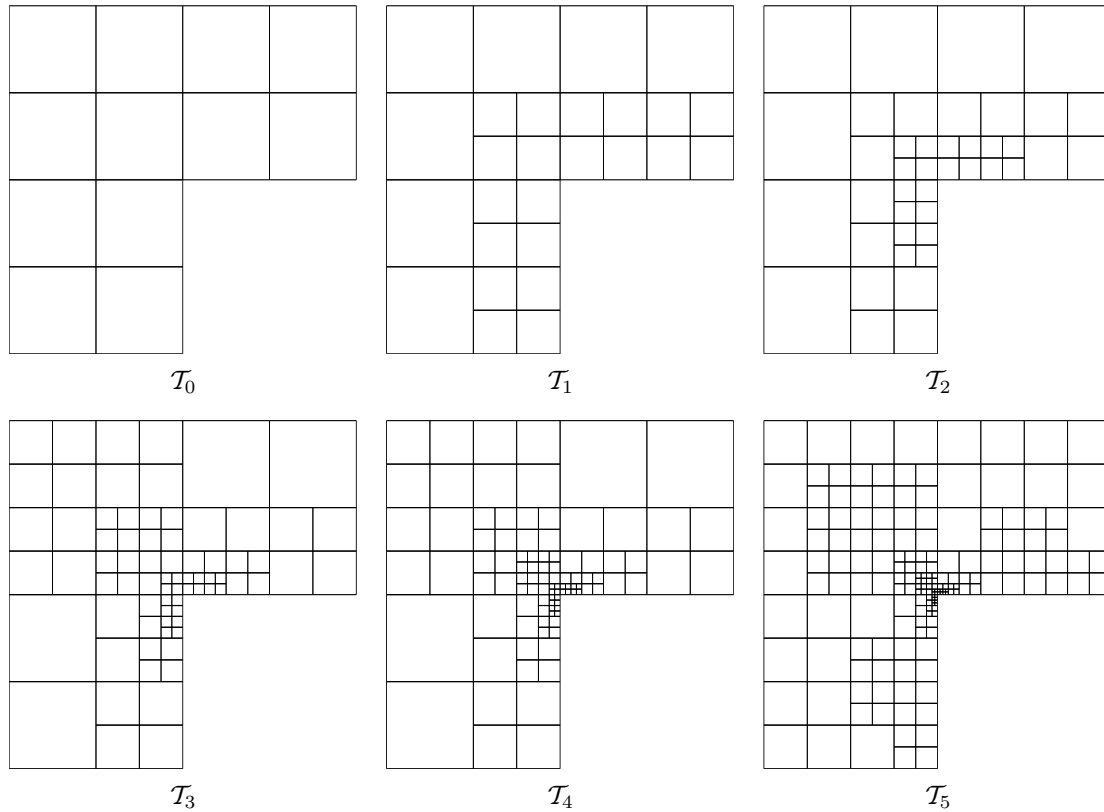


Fig. 5.2. Adapted triangulations $\mathcal{T}_0, \dots, \mathcal{T}_5$ generated with the Algorithm 5.1 with $\theta = 1/2$.

Acknowledgments. The first author CC was supported by DFG Research Center MATHEON “Mathematics for key technologies” in Berlin. The second author JH was supported by the NSFC under Grant 10601003 and A Foundation for the Author of National Excellent Doctoral

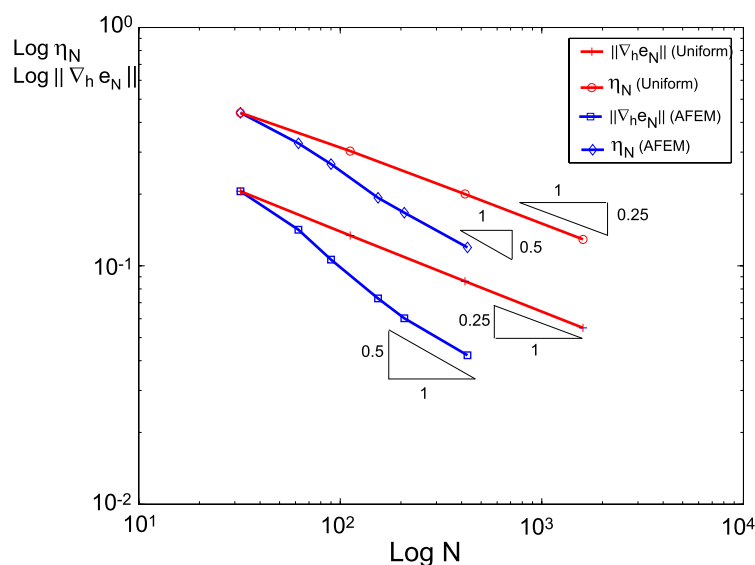


Fig. 5.3. Experimental convergence rate of η_N and the exact error $\|\nabla_h e_N\|$ with respect to the number N of degrees of freedom for the adaptive and uniform refinement based on η_N and with the NR finite element .

Dissertation of PR China 200718. Both authors are corresponding authors and thankful for the support of two Sino-German workshops on Applied and Computational Mathematics held in 2005 and 2007 through the Sino-German office in Beijing.

References

- [1] M. Ainsworth and J.T. Oden, A Posteriori Error Estimation in Inite Element Analysis, John Wiley & Sons, New York, 2000.
- [2] M. Ainsworth, Robust a posteriori error estimation for nonconforming finite element approximation, Preprint, University of Strathclyde (2003).
- [3] M. Ainsworth, A posteriori error estimation for non-conforming quadrilateral finite elements, *Int. J. of Numer. Anal. Mod.*, **2** (2005), 1-18.
- [4] I. Babuska and A. Miller, A feedback finite element method with a posteriori error estimation: Part I. The finite element method and some basic properties of the a posteriori error estimator, *Comput. Method. Appl. M.*, **61** (1987), 1-40.
- [5] I. Babuška and W.C. Rheinboldt, A posteriori error analysis of finite element solutions for 1-dimensional problems, *SIAM J. Numer. Anal.*, **18** (1981), 565-589.
- [6] I. Babuška and T. Strouboulis, The Finite Element Method and its Reliability, The Clarendon Press Oxford University Press, 2001.
- [7] S. Brenner and C. Carstensen, Finite Element Methods, Chapter 4 in Encyclopedia of Computational Mechanics, John Wiley & Sons, 2004.
- [8] R. Becker and R. Rannacher, An optimal control approach to a posteriori error estimation in finite element methods, *Acta Numerica*, 2001, 1-102.
- [9] C. Bernardi and V. Girault, A local regularisation operator for triangular and quadrilateral finite elements, *SIAM J. Numer. Anal.*, **35** (1998), 1893-1916.
- [10] D. Braess, Stability of saddle point problems with penalty, *M²AN*, **30** (1996), 731-742.
- [11] D. Braess, Finite Elements, Cambridge University Press, 1997.

- [12] D. Braess, C. Carstensen and B.D. Reddy, Uniform convergence and a posteriori error estimators for the enhanced strain finite element method, *Numer. Math.*, **96** (2004), 461-479.
- [13] S.C. Brenner and L.R. Scott, The Mathematical Theory of Finite Element Methods, Springer Verlag, 2nd Edition, 2002.
- [14] S.C. Brenner and L.Y. Sung, Linear finite element methods for planar linear elasticity, *Math. Comput.*, **59** (1992), 321-338.
- [15] F. Brezzi and M. Fortin, Mixed and Hybrid Finite Element Methods, Springer, Berlin, 1991.
- [16] Z. Cai, J. Douglas, Jr., and X. Ye, A stable nonconforming quadrilateral finite element method for the stationary Stokes and Navier-Stokes equations, *Calcolo*, **36** (1999), 215-232.
- [17] C. Carstensen, Quasi-interpolation and a posteriori error analysis in finite element methods, *M²AN Math. Model. Numer. Anal.*, **33** (1999), 1187-1202.
- [18] C. Carstensen, A unifying theory of a posteriori finite element error control, *Numer. Math.*, (2005).
- [19] C. Carstensen and S. Bartels, Each averaging technique yields reliable a posteriori error control in FEM on unstructured grids. Part I: Low order conforming, nonconforming, and mixed FEM, *Math. Comput.*, **71** (2002), 945-969.
- [20] C. Carstensen, S. Bartels, and S. Jansche, A posteriori error estimates for nonconforming finite element methods, *Numer. Math.*, **92** (2002), 233-256.
- [21] C. Carstensen, T. Gudi and M. Jensen, A unifying theory of a posteriori error control for discontinuous Galerkin FEM. *Numer Math*, submitted, (2008).
- [22] C. Carstensen and Jun Hu, A unifying theory of a posteriori error control for nonconforming finite element methods, *Numer. Math.*, 107 (2007), 455-471.
- [23] C. Carstensen, Jun Hu and A. Orlando, Framework for the a posteriori error analysis of nonconforming finite elements, *SIAM J. Numer. Anal.*, **45** (2007), 68-82.
- [24] C. Carstensen and S.A. Funken, A posteriori error control in low-order finite element discretisations of incompressible stationary flow problems *Math. Comput.*, **70**:236 (2001), 1353-1381.
- [25] C. Carstensen and J. Schöberl, Residual-Based a posteriori error estimate for a mixed Reissner-Mindlin plate finite element, *Numer. Math.*, **103** (2006), 225-250.
- [26] P.G. Ciarlet, The Finite Element Method for Elliptic Problems, North-Holland, 1978; reprinted as SIAM Classics in Applied Mathematics, 2002.
- [27] M. Crouzeix and P.-A. Raviart, Conforming and nonconforming finite element methods for solving the stationary Stokes equations, *RAIRO Anal. Numér.*, **7** (1973), 33-76.
- [28] E. Dari, R. Duran and C. Padra, Error estimators for nonconforming finite element approximations of the Stokes problem, *Math. Comput.*, **64** (1995), 1017-1033.
- [29] E. Dari, R. Duran, C. Padra and V. Vampa, A posteriori error estimators for nonconforming finite element methods, *Math. Model. Numer. Anal.*, **30** (1996), 385-400.
- [30] J. Douglas Jr, J.E. Santos, D. Sheen and X. Ye, Nonconforming Galerkin methods based on quadrilateral elements for second order elliptic problems, *Math. Model. Numer. Anal.*, **33** (1999), 747-770.
- [31] V. Girault and P.-A. Raviart, Finite Element Methods for Navier-Stokes Equations, Springer Verlag, 1986.
- [32] H.-D. Han, Nonconforming elements in the mixed finite element method, *J. Comput. Math.*, **2** (1984), 223-233.
- [33] J. Hu and Y.Q. Huang, A posteriori error analysis of finite element methods for the Reissner-Mindlin Plates, Preprint document of institute of mathematics of PeKing University, NO.30, 2007.
- [34] J. Hu and Z.-C. Shi, Constrained nonconforming rotated Q_1 -element, *J. Comput. Math.*, **23** (2005), 561-586.
- [35] G. Kanschat and F.-T. Suttmeier, A posteriori error estimates for nonconforming finite element schemes, *Calcolo*, **36** (1999), 129-141.
- [36] C. Park and D. Sheen, P_1 -nonconforming quadrilateral finite element methods for second-order

- elliptic problems, *SIAM J. Numer. Anal.*, **41** (2003), 624-640.
- [37] R. Rannacher and S. Turek, Simple nonconforming quadrilateral Stokes element, *Numer. Meth. Part. D. E.*, **8** (1992), 97-111.
- [38] Z.-C. Shi, A convergence condition for quadrilateral Wilson element, *Numer. Math.*, **44** (1984), 349-361.
- [39] Z.-C. Shi, The FEM-Test for nonconforming finite elements, *Math. Comput.*, **49** (1987), 391-405.
- [40] R. Verfürth, A Review of A Posteriori Error Estimation and Adaptive Mesh-Refinement Techniques, Wiley-Teubner, 1996.